INSTITUTE OF PHYSICS PUBLISHING PHYSICS IN MEDICINE AND BIOLOGY

Phys. Med. Biol. **50** (2005) 5953–5967 doi:10.1088/0031-9155/50/24/013

Method for determination of the mean fraction of glandular tissue in individual female breasts using mammography

J T M Jansen[1], W J H Veldkamp[2], M A O Thijssen[3], S van Woudenberg[3] and J Zoetelief[1]

[1] Department of Radiation, Radionuclides and Reactors, Faculty of Applied Sciences, Delft University of Technology, Mekelweg 15, 2629 JB Delft, The Netherlands
[2] Department of Radiology, Leiden University Medical Center, Albinusdreef 2, 2300 RC Leiden, The Netherlands
[3] National Expert and Training Centre for Breast Cancer Screening, Radboud University Nijmegen Medical Centre, Geert Grooteplein-Zuid 10, 6525 GA Nijmegen, The Netherlands

E-mail: j.t.m.jansen@tnw.tudelft.nl

Received 23 August 2005, in final form 24 October 2005
Published 7 December 2005
Online at stacks.iop.org/PMB/50/5953

Abstract

The nationwide breast cancer screening programme using mammography has been in full operation in the Netherlands since 1997. Quality control of the screening programme has been assigned to the National Expert and Training Centre for Breast Cancer Screening. Limits are set to the mean glandular dose and the centre monitors these for all facilities engaged in the screening programme. This procedure is restricted to the determination of the entrance dose on a 5 cm thick polymethylmethacrylate (PMMA) phantom. The mean glandular dose for a compressed breast is estimated from these data. Individual breasts may deviate largely from this 5 cm PMMA breast model. Not only may the compressed breast size vary from 2 to 10 cm, but breast composition varies also. The mean glandular dose is dependent on the fraction of glandular tissue (glandularity) of the breast. To estimate the risk related to individual mammograms requires the development of a method for determination of the glandularity of individual breasts. A method has been developed to derive the glandularity using the attenuation of mammography x-rays in the breast. The method was applied to a series of mammograms at a screening unit. The results, i.e., a glandularity of 93% within the range of 0 to 1, were comparable with data in the literature. The glandularity as a function of compressed breast thickness is similar to results from other investigators using differing methods.

1. Introduction

The nationwide breast cancer screening programme using mammography has been in full operation in the Netherlands since 1997. The screening is performed in nine regions of the country employing 63 screening units and 28 central reading units. Annually, about one million women in the age group of 50 to 75 years are invited for screening and approximately 80% of the invited women actually participate. About 1% of the participating women are called back for further investigation. In about half of these latter women (4000) cancer is diagnosed.

The National Expert and Training Centre for Breast Cancer Screening (LRCB) performs dosimetry for mammography according to the quality control procedures of the Dutch breast cancer screening programme. The dosimetry is restricted to the determination of entrance dose and mean glandular dose based upon measurements on a 5 cm thick polymethylmethacrylate (PMMA) phantom simulating approximately the average compressed breast. The mean glandular dose, $\overline{D_G}$, is derived from the incident air kerma, $K_{a,i}$, measured without backscatter for the 5 cm thick PMMA phantom according to the method of Dance *et al* (2000):

$$\overline{D_G} = K_{a,i} gcs \tag{1}$$

where g is the incident air kerma to mean glandular dose conversion factor, c is a correction factor for any difference in breast composition from 50% glandularity and s is a correction factor for any difference in the x-ray spectrum from that produced by an x-ray tube with a molybdenum (Mo) anode and a Mo filter operated at a tube voltage of 28 kV. The correction for glandularity is based on an average value determined as a function of compressed breast thickness and age.

The LRCB employs a 5 cm thick PMMA phantom for determining the mean glandular dose. PMMA simulates the composition at approximately average breast thickness containing a central region of average composition, i.e., about 50% glandular tissue and 50% adipose tissue. Individual breasts may deviate considerably from this PMMA model, in thickness as well as composition (fraction of glandular tissue, glandularity). For the implementation of a population breast cancer screening programme using mammography it is a prerequisite that the benefits of screening are considerably larger than the risks induced due to the use of ionizing radiation. To derive the risks related to individual mammograms, therefore, the breast thickness has to be determined and the development of a method for determination of mean glandularity for individual mammograms is required. A method has been presented by Highnam *et al* (1998), employing the attenuation of mammography x-rays in the female breast to determine the fraction of glandular tissue. They also reported to be able to derive the compressed breast thickness from a region were the full thickness of the breast was only consisting of adipose tissue, i.e., containing only the skin and underlying adipose tissue.

The present study was performed to investigate if a method based on that published by Highnam *et al* (1998) can be used in practice for determination of glandularity (the mean fraction of glandular tissue) of individual breasts in the Dutch breast cancer screening programme. The adapted method has been applied to a series of mammograms produced at a screening unit. An additional motivation to determine the glandularity is a possible correlation between breast density and breast cancer risk (Yaffe and Boyd 2005).

2. Materials and methods

The method used to derive glandularity of individual compressed breasts during mammography and eventually the mean glandular dose for a compressed breast in the case of mammography requires various steps, which are presented below in separate subsections.

2.1. Determination of air kerma free-in-air from x-ray tube output

Air kerma, K_a, can be derived from the calibration of x-ray tube output, Y, at a specified distance from the focus in terms of air kerma free-in-air per unit of tube current-exposure time product in units of Gy $(\mathrm{mAs})^{-1}$. The specified distance is taken as 1 m by convention. When the tube current-exposure time product is known the air kerma free-in-air at 1 m from the focus of the x-ray tube follows. It is noted that during the calibration of the x-ray tube output the compression plate must be present in the beam. For a common x-ray tube output measurement this is not the case and our values will, therefore, be lower than published values due to the attenuation of x-rays in the compression plate.

For measurement of the x-ray tube output of a specific mammography unit it is sufficient to specify the radiation quality only by the anode/filter combination and the tube voltage. The x-ray tube output has to be measured at all relevant settings of radiation quality.

2.2. Determination of compressed breast thickness

Determination of the compressed breast thickness for each image is necessary to determine incident air kerma, to relate measured and calculated attenuation in the compressed breast and to apply an appropriate conversion factor from air kerma to mean glandular dose. It is well known (Burch and Law 1995) that the indication of breast thickness on mammography units is not always reliable, since the compression plate can deform considerably. Burch and Law have proposed a thickness measurement based on the imaging of lead markers placed on the compression plate and by calibration of the breast thickness on the imaged positions of the lead markers. This method has been applied in the present study for determination of the compressed breast thickness.

2.3. Incident air kerma on the compressed breast per mammogram

With known focal point-to-(breast) surface distance, d_{FSD} (which is derived from the focus to breast support table distance and the compressed breast thickness), the incident air kerma on the compressed female breast, $K_{a,i}$ can be derived according to

$$K_{a,i} = d_{\mathrm{FSD}}^{-2} Y Q \tag{2}$$

where Q is the tube current-exposure time product for an individual image and Y is the x-ray tube output for the relevant radiation quality, i.e., anode/filter combination and tube voltage for a specific mammography unit. For each mammogram, the tube current-exposure time product, Q, as well as d_{FSD}, i.e., d_{F-T} and compressed breast thickness, t, have to be obtained to derive the incident air kerma per mammogram according to equation (2). In addition, the anode/filter combination and the applied tube voltage have to be known to apply the correct x-ray tube output Y.

2.4. Mean glandular dose per mammogram

The mean glandular dose per mammogram can be determined using an equation similar to equation (1) except that correction factors are not needed when the conversion factor g is determined as a function of compressed breast thickness, t, the glandularity of the breast, p, and for the actual anode/filter combinations, a/f, and tube voltages, V_T, used, $g(t, p, a/f, V_T)$:

$$\overline{D_G} = K_{a,i} \quad g(t, p, a/f, V_T). \tag{3}$$

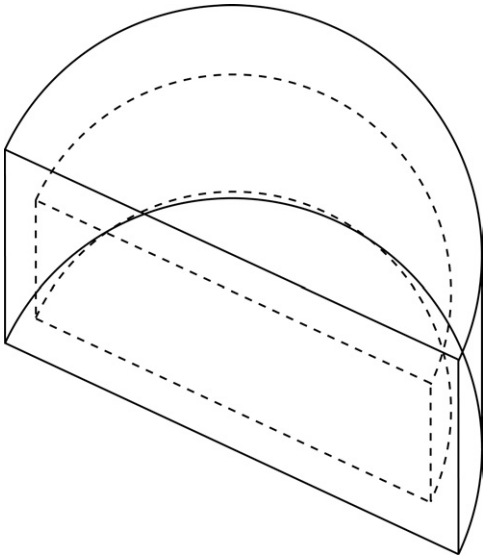

Figure 1. A schematic drawing of the compressed breast model with the central part simulating the breast tissue as half a cylinder enclosed by the dashed lines and the outer part simulating skin and underlying adipose tissue enclosed by the dashed lines from the inside and the solid lines from the outside.

2.5. Calculation of attenuation in the breast (model) and of conversion coefficients $g(t, p, a/f, V_T)$

To calculate the attenuation in the female breast, the Monte Carlo *N*-particle radiation transport code, MCNP (Briesmeister 2000), was used. The total number of starting photons for each simulation was 200 million, to get statistically reliable results in a reasonable processor time. The mathematical model will be described in detail below.

The compressed female breast was modelled as half a cylinder with a radius of 8 cm. The cylinder was cut in half along the central cylinder axis. The central part simulates the breast tissue and the outer part of the compressed breast model simulates the skin and underlying adipose tissue, see figure 1 (Dance, 1990, Hammerstein 1979). The outer layer is situated in the top and bottom plane of the cylinder and in the curved part of the cylinder. For the central region three compositions have been used, i.e., 100% adipose tissue, a mixture of 50% adipose tissue and 50% glandular tissue by mass and 100% glandular tissue. The outer part of the compressed breast model is mimicked using three approaches. The first is by a 5 mm thick homogeneous adipose tissue layer, as proposed by Dance (1990), the second by a homogeneous 5 mm thick layer of glandular tissue and the third by a two component model, i.e., 3 mm adipose tissue covered by 2 mm skin tissue. The overall breast thickness is varied and values of 11, 20, 30, 40, 50, 60, 70, 80, 90, 100 and 110 mm have been used.

In addition, calculations have been made with half cylinders made out of air or PMMA. The calculations with air are performed to derive the entrance dose without backscatter. The calculations for PMMA are performed to derive the attenuation in the PMMA phantom in a similar way as for the breast model.

The attenuation or elemental composition of the tissues in the female breast and their densities are taken from three sources, namely either ICRU Report 44 (ICRU 1989), Hammerstein *et al* (1979) and Highnam and Brady (1999). For Highnam and Brady, no tissue

Table 1. Linear attenuation coefficients for glandular tissue and adipose tissue according to various references.

Photon energy	Glandular tissue			Adipose tissue		
E (keV)	μ_{int}[a] (cm^{-1})	μ_{breast}[b] (cm^{-1})	μ_{gland}[c] (cm^{-1})	μ_{fat}[a] (cm^{-1})	μ_{adipose}[b] (cm^{-1})	μ_{adipose}[c] (cm^{-1})
15	1.635	1.408	1.54	0.832	1.026	0.92
20	0.802	0.703	0.747	0.456	0.540	0.499
30	0.374	0.347	0.364	0.263	0.291	0.274

[a] Highnam and Brady (1999) based on measurements of Johns and Yaffe (1987).
[b] ICRU 44 (1989).
[c] Hammerstein *et al* (1979).

composition is supplied but attenuation coefficients are measured by Johns and Yaffe (1987) at photon energies of 18, 20, 25, 30, 40, 50, 80 and 110 keV. Hammerstein *et al* give the results on elemental composition and density for various samples. Also the ICRU (1989) provides data on elemental composition and density for various tissues in the female breast. The program XCOM (Berger and Hubbell 1999) is used to calculate the attenuation coefficients for the elementary compositions provided by Hammerstein *et al* and the ICRU. All three sources specify data for adipose tissue and glandular tissue. Hammerstein *et al* and ICRU Report 44 specify in addition the composition and density of the skin. Highnam and Brady, and Johns and Yaffe do not provide linear attenuation coefficients for skin. Therefore, in the case of the use of linear attenuation coefficients of Highnam and Brady, the skin compositions and derived attenuation coefficients of the ICRU are used when applicable. The linear attenuation coefficients according to the various sources of information are given in table 1.

The mammography units used have a Mo anode and a Mo filter of 0.030 mm thickness. For the unit used to test the method in more detail a Rh filter of 0.025 mm thickness is also present. The x-ray spectra are calculated employing IPEM software Report 78 (1997) for an anode angle of 16° and no ripple on the tube voltage. The tube voltages used are 25, 28 and 31 kV, for both anode filter combinations. The distance from focus to breast support table is 60 cm. The focus is positioned 0.01 mm from the central cylinder axis, towards the centre of the breast phantom, to avoid possible problems at interfaces of cells. The central beam axis is perpendicular to the top surface of the phantom. The x-ray beam is a half cone with a field radius of 8 cm at 48 cm distance from the focus and the focus is an isotropic point source restricted to emission inside the beam.

The compression paddle is made of PMMA and has a thickness of 2 mm in the beam direction and 10 cm and 20 cm as the other dimensions. To calculate the entrance and exit absorbed dose to air or air kerma an air layer of 0.01 mm air has been added between the compression paddle and the phantom and between the phantom and the breast support table. The entrance and exit absorbed dose to air or air kerma are calculated as average over the whole cell by applying a fluence to absorbed dose in air conversion coefficient based on NISTIR 5632 (NIST 1995) or a fluence to air kerma conversion coefficient based on ICRU Report 47 (ICRU 1992). For NISTIR 5632 (NIST 1995) the lowest photon energy, where a conversion coefficient is available, is 1 keV and for ICRU Report 47 this is 10 keV. In the photon energy range from 10 keV to 40 keV, the conversion coefficients according to ICRU Report 47 (1992) are between 2% to 3% lower than that in NISTIR 5632. In addition, values for attenuation were calculated for a PMMA phantom.

The conversion coefficients $g(t, p, a/f, V_T)$ were calculated previously as published by Klein *et al* (1997). The breast model used is that proposed by Dance (1990) and Hammerstein *et al* (1979), consisting of the central region of a mixture of glandular and adipose tissue and

a superficial layer of 0.5 cm of adipose tissue representing skin and underlying adipose tissue. Tissue compositions of Hammerstein *et al* (1979) were used.

2.6. Determination of the actual attenuation in a female breast for an individual mammogram

To determine the attenuation at various positions in the compressed breast all images were digitized. The air kerma per pixel of the mammogram (in front of the anti-scatter grid and the film–screen combination) is determined from the optical density using a calibrated film digitizer. This calibration is performed by measuring air kerma behind PMMA phantoms of various thicknesses, i.e., the exit air kerma. The exit air kerma for mammograms was corrected for heel effect using a correction image. The correction image was obtained from recordings of a uniform 4 cm thick PMMA layer. A correction value was obtained for each pixel by dividing the actual pixel value by the value at a predefined reference point. Pixel values of a real mammogram were corrected with the correction image before determination of the exit air kerma. For determination of the attenuation a correction was made for sagging of the compression plate for the entrance dose at each pixel location. The degree of sagging at the centre of gravity of the mammographic area was determined. This value was subtracted from the breast thickness and taken into account for calculating entrance exposure.

The LRCB has performed their quality control measurements and additional measurements the week before the two weeks period in which the films and the x-ray machine parameters as filter material, tube voltage and tube current-exposure time product were collected. All screening units process a sensitometric step-wedge as part of their daily quality control (Beckers *et al* 2003). During the LRCB quality control measurements all available cassettes on a screening unit are checked for differences in sensitivity and exposure difference. This is performed with a 5 cm thick PMMA block placed on the bucky with the dosimeter next to the reference point and the automatic exposure control (AEC) setting to obtain a density between 1.0 and 1.2 OD. The dose close to the reference point is recorded, the images are processed, and the density in the reference point is measured. The variation in optical density is smaller than or equal to 0.15 OD and preferably smaller than 0.10 OD. The dose for a density of 1.00 OD above base and fog is calculated (Beckers *et al* 2003) and the variation is less than or equal to 10%. During the period when the actual measurements were taken, the unit was under daily QC. This ensures that the variation in speed remains below 0.03, and the radiation dose within 5% for the 5 cm PMMA block at the given AEC setting. Also the OD obtained remains within 0.15 OD, for the given period.

The x-ray tube output is measured using an ionization chamber as described in section 2.1. The actual attenuation is obtained as the exit air kerma divided by the incident air kerma for the compressed female breast. In addition to the measurement of the exit air kerma for each filter and tube voltage used for various thicknesses of PMMA phantom, images were made without the ionization chamber. These images are digitized and used to calibrate the optical density to exit kerma for a breast during mammography on pixel-by-pixel bases. It should be borne in mind that the relationship between the optical density and the exit absorbed dose to air or air kerma is dependent on the compressed breast or phantom thickness. For thicker objects more scattered radiation is produced in the compressed breast or phantom and consequently absorbed in the anti-scatter grid. The correction factor to be applied on the optical density to account for the increase in the production of scattered radiation with increasing compressed breast thickness is measured and presented in table 2. This method is chosen to avoid the need to simulate the anti-scatter grid in the attenuation calculation and the heel effect. These phenomena are now corrected for by the pixel-by-pixel calibration. Although with increasing glandularity of the breast the scatter contribution increases, this contribution is much smaller

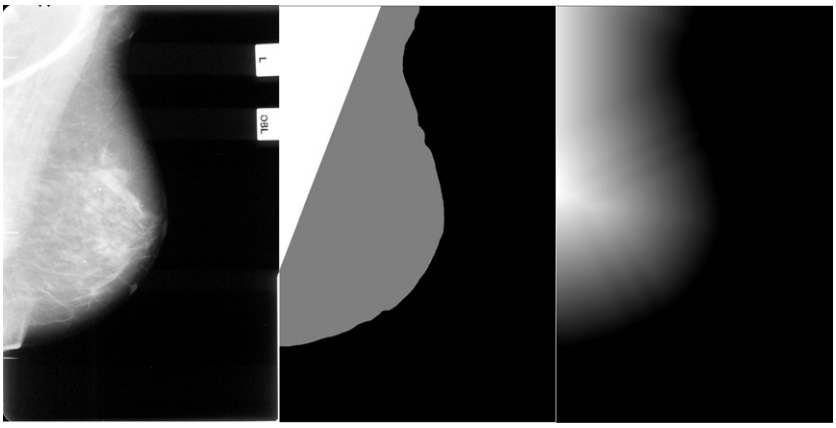

Figure 2. A left oblique mammogram is shown in the left panel. This mammogram is segmented with a mask (grey), excluding the pectoral muscle (white) and the region outside of the breast (black), as is shown in the middle panel. In the right panel the distance transform of the mammogram is shown for the whole breast region, including the pectoral muscle. Grey values in the whole breast region indicate the distance of this pixel to the outer region of the breast, with white for large and black for close distances. Pixels outside the whole breast region are in black.

Table 2. Scatter correction factor as a function of compressed breast thickness as determined from measurements for phantoms of varying thickness. The values are given with reference to a compressed breast thickness of 5 cm.

Breast thickness (cm)	Scatter correction
1.1	0.81
2.0	0.87
3.0	0.94
4.0	0.97
5.0	1
6.0	1.04
7.0	1.08
8.0	1.13
9.0	1.18
10.0	1.23
11.0	1.28

than for the thickness. A roughly estimated correction factor taking into account the effects of using grids would be between 0.98 and 1.02 and this is so close to 1 that the correction is neglected.

The outer regions of the mammogram will include predominantly skin and underlying adipose tissue, whereas the thickness in these regions may be smaller than the compressed breast thickness. It has been decided, therefore, to exclude a fraction of the breast region of the mammogram as an outer layer. A distance transform was used for this purpose. The initial segmentation of background from tissue area is performed using a global thresholding technique on the mammogram. The mammogram is shown in the left panel of figure 2. The border between tissue (including skin and not necessarily having the complete breast thickness) and air is shown in the middle panel of figure 2 as the jump in grey value from black to grey. The border between the pectoral muscle and breast tissue is shown in the middle panel of figure 2 as the jump in grey value between white and grey. This segmentation is performed

based on the prior knowledge that it should be a straight line and that the gradient magnitude should be high (Karssemeijer). After this segmentation the distance transform is performed, with the pectoral muscle area included in the distance transform. The distance transform is an operator normally only applied to binary images (foreground = 1, background = 0). The result of the transform is a grey-level image where the grey-level intensity of points inside foreground regions indicates the distance to the closest boundary from each point (Jain 1989). In the right panel of figure 2, the distance transform is shown with white values for large and black values for small distances from the breast edge. The distance transform is applied to the segmented breast area (after exclusion of the pectoral muscle from the breast area). The region at the breast edge that is excluded from further analysis is called the outer region and is defined as 2, 5, 7, 10 and 15% of the maximum distance from the breast edge. The estimated glandularity increases with increasing excluded percentage of the maximum distance from the breast edge. The difference in estimated glandularity between 10 and 15% is the smallest although the percentage difference is the largest and the difference is really small therefore 15% has been chosen as optimal. The segmentation of the breast is described extensively by Karssemeijer (1998).

The actual attenuation was also determined for a PMMA phantom of 4 cm thickness to be compared to calculated attenuation as a first test of the method for an object of known composition.

2.7. Determination of the compressed breast thickness, according to Highnam and Brady

The initial segmentation of the mammogram to determine the breast edge is performed as described in the previous paragraph. Bounds on the breast thickness are determined from the minimal and maximal attenuation values in an area that is completely inside the breast and assuming glandularity 0 and 1, respectively. Assume the lower value for the breast thickness. Apply a correction for the scatter radiation based on this thickness. Find all pixels with glandularity equal to 0 and make a curve. Calculate the roughness of the curve. If the roughness is above the threshold then decrease the thickness and stop, otherwise increase the thickness with 0.1 cm and again apply a scatter radiation correction and so on. This method is checked by comparing it with the thickness method described in paragraph 2.2. In our study, the method of Highnam and Brady failed because there was not an area of uniform compressed breast thickness with a composition of 100% adipose tissue. This is an assumption made in the protocol above. Therefore, the sudden raise of the roughness parameter as described before is not observed. This sudden raise is necessary to determine the threshold to stop the iteration.

2.8. Determination of glandularity for an individual compressed breast during mammography

The glandularity of a breast imaged in the national screening programme at a particular mammography unit can be obtained by using the actual attenuation over the region of interest in the mammogram (section 2.6). For each pixel of the mammogram in the region of interest, as determined by the segmentation of the pectoral muscle and the outer region of the breast on the mammogram, the attenuation is determined. For all pixels of a mammogram the attenuation is stored as a histogram. The attenuation per pixel is compared with the tabulations obtained as described in section 2.5 to derive the glandularity per pixel. The averaged value for the glandularity over the whole histogram is used to derive the mean glandularity of the breast.

As a first test of the method, imaging and Monte Carlo calculations for a 4 cm thick PMMA phantom were used, i.e., comparing results of the methods presented in sections 2.5 and 2.6, using the composition of PMMA according to the ICRU (1989).

2.9. Application of the method for determination of the glandularity of female breasts screened at a unit of the national breast cancer screening

In the first instance calculated attenuation (section 2.5) and actual attenuation (section 2.6) are compared as described in section 2.8 for a rectangular 4 cm thick PMMA phantom. When it was concluded that most likely a successful method was obtained, this was tested for a series of 248 images produced during a week at a screening unit in Arnhem.

When a decision was made on the attenuation coefficients to be used (Highnam and Brady) and on the simulation of skin and underlying adipose tissue, more extended measurements were made on specific screening centre in Arnhem, operating a mammography unit that employs both a Mo/Mo and a Mo/Rh anode filter combination, at tube voltages of 26 to 28 kV and 29 to 31 kV, for Mo/Mo and Mo/Rh, respectively. The unit automatically selects the tube voltage and filter after a small pre-exposure. In total 478 images were analysed involving 259 women.

3. Results

3.1. Results for attenuation calculated in the female breast

For various breast models and various breast thicknesses both entrance and exit doses were calculated using fluence to air kerma coefficients published in ICRU Report 47 (ICRU 1992) and using fluence to dose to air coefficients published in NISTIR 5632 (NIST 1995). The differences between the air kerma calculated with ICRU Report 47 and the dose to air calculated with NISTIR 5632 are between 2.6 and 3.4%, the air kerma values being lower. These differences are somewhat larger than expected, but might be attributed due to photons below 10 keV, as the Monte Carlo transport threshold for photon energy is 1 keV and data in NISTIR 5632 are starting at photon energies of 1 keV whereas in ICRU Report 47 data are only available at photon energies of 10 keV and higher. Therefore, for all further calculations NISTIR 5632 coefficients were used.

The differences between the various breast models with respect to skin and underlying adipose tissue modelled by adipose tissue, glandular tissue or the two-compartment model (skin and adipose tissue) are investigated in terms of entrance and exit doses. The entrance dose to air is between 1 and 4% lower for the glandular tissue layer compared to the adipose tissue layer. For the two-compartment model the entrance dose to air is between 1 and 3% lower than for the adipose tissue layer. For the exit dose to air the differences are larger and the use of glandular tissue results in a lower dose, i.e., between a factor of 0.52 to 0.88 times the value obtained using adipose tissue as a skin model for various breast thicknesses and tissue compositions. For the two-compartment skin model the corresponding factors are between 0.67 and 0.90. If the breast thickness increases the factors approach the higher values. This can be explained by the increased beam hardening for larger breast thicknesses resulting in less attenuation in the different models for skin and underlying adipose tissue models.

Entrance and exit doses to air are calculated using linear attenuation coefficients based on the tissue compositions of ICRU Report 44 (ICRU 1989) and of Hammerstein *et al* (1979), as well as the linear attenuation coefficients of Highnam and Brady (1999), for all breast models and various breast thicknesses and glandularities. The attenuation of a breast model in which skin and underlying adipose tissue is simulated by 5 mm of adipose tissue are shown in figure 3 as a function of the breast thickness for different compositions of the central region, i.e., 0% glandular tissue ($f_g = 0$) and 100% glandular tissue ($f_g = 1$) and the linear attenuation coefficients from the three different sources. The differences in entrance dose using the

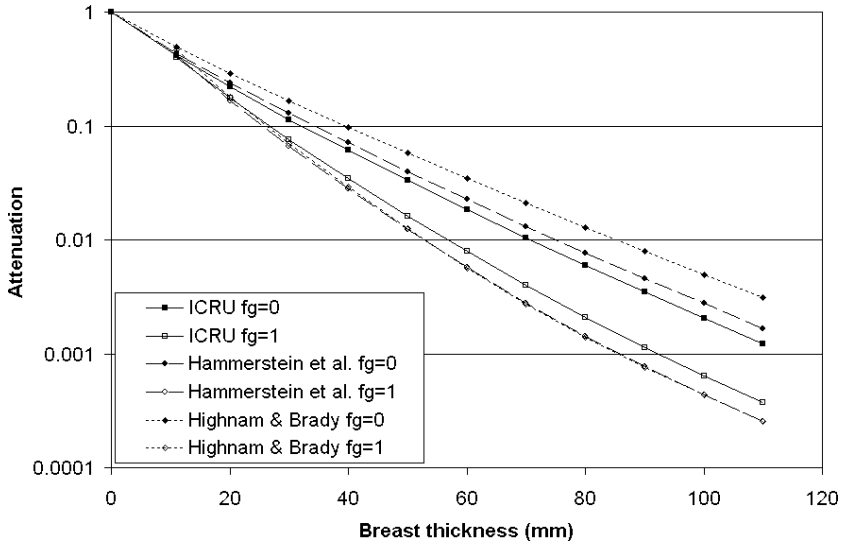

Figure 3. Attenuation (exit dose divided by entrance dose) in a breast model with various breast thicknesses, a superficial layer of 5 mm adipose tissue employing various linear attenuation coefficients for adipose tissue and glandular tissue, i.e., based upon ICRU Report 44 (ICRU 1989), Hammerstein *et al* (1979) and Highnam and Brady (1999). The used spectrum was Mo anode with a Mo filter operated at a tube voltage of 28 kV, according to IPEM 78.

different sources of linear attenuation coefficients are small and within 1% for Hammerstein *et al* and from −1 to +2% for Highnam and Brady compared to ICRU Report 44. For exit dose the differences are considerable, i.e., a ratio of 0.54 to 1.40 for Hammerstein *et al* and a ratio of 0.47 to 2.79 for Highnam and Brady compared to ICRU-44. Both Hammerstein *et al* and Highnam and Brady give for not too thin breasts more attenuation if the glandularity is close to 1 and less attenuation if the glandularity is close to 0 (see figure 3).

Monte Carlo calculations of attenuation have been performed for a number of parameter values, i.e., breast thicknesses of 11, 20, 30, 40, 50, 60, 70, 80, 90, 100 and 110 mm, glandularities of 0, 0.5 and 1, tube voltages of 25, 28 and 31 kV and Mo/Mo and Mo/Rh anode/filter combinations. Because values of attenuation may be needed for parameter values that are not tabulated, it has been investigated which interpolation method, i.e., linear–linear, linear–logarithmic, logarithmic–linear, logarithmic–logarithmic or linear–reciprocal, gives the best results. Therefore, the deviation is determined as the interpolated attenuation minus the calculated attenuation divided by the calculated attenuation times 100%. For breast thickness in the range from 20 to 100 mm, linear–logarithmic interpolation from neighbouring values gave the best results with a minimum deviation of −0.3% and a maximum deviation of 6.9% for all glandularities, breast models, tissue compositions and spectra used. The smallest deviation for obtaining an attenuation value at glandularity of 0.5 was obtained for linear–logarithmic interpolation showing deviations of at minimum −0.4% and at maximum 29%. Linear–logarithmic interpolation is also the preferred method for interpolation of tube voltage at 28 kV from values calculated at 25 and 31 kV with a minimum deviation of −4.2% and a maximum deviation of 2.6%. In practice, the deviations are expected to be considerably smaller as the values at which calculations were made are used. For the glandularity the deviation is the largest and quite non-uniform. The largest deviation of 29% is found for attenuation employing Highnam and Brady attenuation coefficients for a 110 mm thick breast, adipose tissue representing skin and the underlying adipose tissue layer and a tube voltage of

25 kV with a Mo-filter. Such a low tube voltage for such a thick breast is not applicable in practice. For a breast thickness of 80 mm, linear–logarithmic interpolation from glandularity 0 and 1 and all spectra the maximum deviation is 11%. As in practice the glandularity of 0.5 is used as a reference value but not as an interpolated value, this will reduce the deviation in the attenuation to an acceptable level.

The attenuation obtained by Monte Carlo calculation for various breast thicknesses, tube voltages, filter materials and glandularities is shown in table 3. Values of attenuation at tube voltages, breast thicknesses and glandularities not present in the table are obtained by linear–logarithmic interpolation from attenuation at the nearest neighbouring values. This table is used to derive the mean individual glandularity of a female breast from measured attenuation.

3.2. Results obtained for a 4 cm thick PMMA phantom

Initial results for deriving the thickness of a PMMA phantom from measured attenuation (according to sections 2.6 and 2.8) and calculated attenuation (according to section 2.5) are encouraging. The difference between the real thickness of 40 mm and the thicknesses obtained by comparing measured and calculated attenuation, i.e., 39.2 and 40.0 mm was approximately 0.5 mm. It should be borne in mind that for compressed breasts during mammography the situation is different since the breast thickness is known and the composition (glandularity) is unknown. These encouraging results are not a true validation of the method. For a true validation, models of breasts or breasts with known glandularity would be needed for comparison with the derived glandularity according to the method presented here.

3.3. Initial results for deriving the glandularity of compressed female breasts

At a regional breast cancer screening unit 248 images were made and they were analysed according to the procedure described in sections 2.6 and 2.8 to obtain the actual attenuation. To derive the glandularity, the actual attenuation was compared to the calculated attenuation using the various breast models (various skin representations) and the three sources of attenuation coefficients, i.e., ICRU Report 44, Hammerstein *et al* and Highnam and Brady (table 1).

Initially, it was assumed that the tissue compositions of the ICRU were most reliable, since contrary to the breast samples analysed by Hammerstein *et al*, samples possibly containing tumour material were excluded from the chemical analysis. Consequently, the linear attenuation coefficients in table 1 according to the ICRU were used to calculate attenuation. When measured and calculated attenuation were used to derive glandularity, 29, 60 and 93% of breasts appeared to have a glandularity between 0 and 1 for the ICRU, Hammerstein *et al* and Highnam and Brady, respectively. To get physically realistic values for the individual breasts, mean glandularity should be between 0 and 1. Therefore, the Highnam and Brady data are preferred. An additional reason for glandularities lower than 0 and larger than 1 is that in this study an average composition is assumed for adipose and glandular tissue although individual variations cannot be excluded (Hammerstein *et al* 1997, ICRU 1989, Johns and Yaffe 1987).

The attenuation as a function of compressed breast thickness for adipose tissue and glandular tissue in figure 3 shows relatively small differences for attenuation derived from ICRU Report 44 (ICRU 1989). This implies that a difference in glandularity has only a marginal influence. The attenuation curves for adipose tissue and glandular tissue in figure 3 show considerably larger differences for the attenuation of Highnam and Brady (1999). The linear attenuation coefficients of Highnam and Brady were also used by Highnam *et al* (1998).

Table 3. Attenuation obtained by Monte Carlo calculation as exit dose to air divided by entrance dose to air using fluence to dose to air coefficients of NISTIR 5632 (NIST 1995). The breast model contains a 5 mm adipose tissue layer to represent skin and underlying adipose tissue. Attenuation coefficients according to Highnam and Brady (1999) for adipose and glandular tissues are used. Attenuation is given for various filter materials and a Mo anode, tube voltages and compositions of the central part of the breast model, i.e., glandularities of 0, 0.5 and 1.

	Filter material																	
	Mo	Mo	Mo	Mo	Mo	Mo	Mo	Mo	Mo	Rh	Rh	Rh	Rh	Rh	Rh	Rh	Rh	Rh
	Tube voltage (kV)																	
	25	25	25	28	28	28	31	31	31	25	25	25	28	28	28	31	31	31
	Glandularity																	
	0	0.5	1	0	0.5	1	0	0.5	1	0	0.5	1	0	0.5	1	0	0.5	1
	Attenuation																	
Breast thickness (mm)																		
11	0.461	0.448	0.433	0.490	0.477	0.462	0.511	0.498	0.484	0.508	0.495	0.481	0.537	0.523	0.510	0.554	0.541	0.527
20	0.263	0.204	0.158	0.289	0.228	0.179	0.309	0.246	0.196	0.307	0.244	0.195	0.333	0.269	0.217	0.350	0.285	0.231
30	0.147	0.092 4	0.059 2	0.166	0.107	0.070 4	0.181	0.120	0.079 8	0.180	0.120	0.080 4	0.201	0.136	0.093 2	0.214	0.147	0.102
40	0.083 9	0.043 7	0.023 5	0.097 5	0.052 6	0.029 1	0.108	0.060 1	0.034 4	0.108	0.060 8	0.035 1	0.123	0.071 1	0.042 0	0.133	0.077 8	0.046 8
50	0.048 8	0.021 3	0.009 61	0.058 0	0.026 3	0.012 5	0.065 6	0.031 1	0.015 5	0.066 0	0.031 8	0.015 9	0.076 4	0.038 0	0.019 6	0.083 1	0.042 3	0.022 4
60	0.028 8	0.010 6	0.004 14	0.034 8	0.013 6	0.005 68	0.040 2	0.016 6	0.007 51	0.040 7	0.017 0	0.007 50	0.047 9	0.020 8	0.009 55	0.052 5	0.023 6	0.011 3
70	0.017 1	0.005 39	0.001 89	0.021 1	0.007 17	0.002 74	0.024 8	0.009 14	0.003 88	0.025 3	0.009 31	0.003 68	0.030 2	0.011 7	0.004 84	0.033 6	0.013 5	0.005 95
80	0.010 2	0.002 79	0.000 905	0.012 9	0.003 88	0.001 40	0.015 5	0.005 18	0.002 15	0.015 9	0.005 17	0.001 87	0.019 2	0.006 62	0.002 54	0.021 6	0.007 87	0.003 27
90	0.006 17	0.001 49	0.000 463	0.007 98	0.002 17	0.000 757	0.009 79	0.003 04	0.001 25	0.010 0	0.002 93	0.000 982	0.012 3	0.003 84	0.001 38	0.014 0	0.004 69	0.001 86
100	0.003 76	0.000 805	0.000 257	0.004 95	0.001 24	0.000 435	0.006 25	0.001 85	0.000 760	0.006 40	0.001 68	0.000 533	0.007 94	0.002 26	0.000 767	0.009 13	0.002 85	0.001 08
110	0.002 28	0.000 446	0.000 146	0.003 10	0.000 720	0.000 254	0.004 02	0.001 15	0.000 466	0.004 07	0.000 968	0.000 297	0.005 15	0.001 35	0.000 437	0.006 02	0.001 76	0.000 647

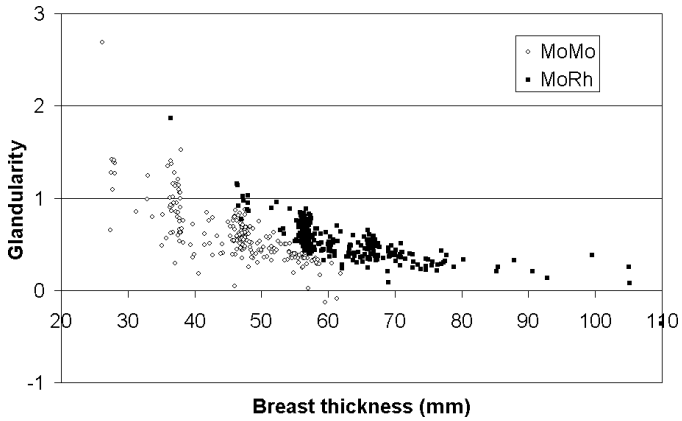

Figure 4. Glandularity as a function of compressed breast thickness obtained from attenuation measurement and calculation at a screening unit of the Netherlands breast cancer screening unit in Arnhem. Differences are observed for the Mo/Mo compared with the Mo/Rh anode /filter combination.

Therefore, it was decided to use the attenuation coefficients from Highnam and Brady for further calculations. In addition, it was decided to use the breast model with skin and underlying adipose tissue being simulated by a layer of 5 mm of adipose tissue, since this model is most widely used.

When the 248 images were analysed using the attenuation obtained with the linear attenuation coefficients from Highnam and Brady, for the breast model using a superficial layer of 5 mm of adipose tissue, it appeared that 93% of the compressed breasts glandularities appeared to be in the range of 0 to 1. Only 2% average compressed breast glandularities larger than 1 and 5% smaller than 0 were encountered. Similar observations were made by other investigators, e.g., Klein *et al* (1997).

Attempts to find a region where the compressed breast consists of adipose tissue (and skin) over the total breast thickness failed both for locations near the edge of the compressed breast and for a location near the pectoral muscle. Consequently, a method similar to that used by Highnam *et al* (1998) (section 2.7) for assessment of the total breast thickness was not applicable.

3.4. Results from a production at a relatively modern mammography unit in Arnhem of the national screening programme

More extended measurements were made on a mammography unit that employs a Mo/Mo or a Mo/Rh anode filter combination, at tube voltages of 26 to 28 kV and 29 to 31 kV, for Mo/Mo and Mo/Rh, respectively. The tube voltage and filter are selected automatically after a small pre-exposure. In total 478 images were made involving 259 women. About 49% of the mammograms were made with the Mo/Mo anode filter combination and 51% with Mo/Rh. The results of the production in Arnhem are shown in figure 4. The mean glandularity for the individual compressed breasts is in approximately 1% of the cases below 0, in 93% of the cases between 0 and 1 and in 6% of the cases above 1. The glandularity as a function of compressed breast thickness is similar to published results using another method (Klein *et al* 1997).

The selection of the Mo/Mo anode filter combination is expected in the case of small compressed breast thicknesses and for low glandularities. The selection of the Mo/Rh anode

filter combination is expected in the case of larger compressed breast thicknesses and for larger glandularities. Figure 4 shows that the selection of the anode/filter combinations is as expected. For approximately average compressed breast thicknesses, i.e., 5 to 6 cm Mo/Mo is used for lower glandularity and Mo/Rh for larger glandularity.

When the conversion coefficients $g(t, p, a/f, V_T)$ as published by Klein *et al* (1997) were used to calculate the average value of the mean glandular dose for the women investigated at the mammography unit a value of 1.7 mGy resulted with a standard deviation of 0.7 mGy. These values are only approximations as the interaction coefficients according to Highnam and Brady should be used instead of that of Hammerstein *et al* (1979). It should be noted that the data for glandular tissue of Hammerstein *et al* and Highnam and Brady are similar (figure 3). The average value of the mean glandular dose and the standard deviation are quite reasonable compared to published values, e.g., Klein *et al* (1997).

4. Conclusions

A method has been developed to determine the glandularity for individual compressed breasts during mammography, based on measurement and calculation of attenuation, similar to the approach proposed by Highnam *et al* (1998). A procedure to determine the compressed breast thickness proposed by Highnam *et al* (1998) could not be made operational, due to the lack of an identifiable area composed of only adipose tissue and skin and of the complete compressed breast thickness.

The adipose tissue and glandular tissue compositions of ICRU Report 44 (ICRU 1989) and those of Hammerstein *et al* (1979) and their derived linear attenuation coefficients are incompatible with obtaining glandularities that are predominantly in the range of 0 to 1, which makes sense physically. Only the linear attenuation coefficients published by Highnam and Brady (1999) provide satisfactory results.

An accurate method for measurement of the compressed breast thickness, such as proposed by Burch and Law (1995), is crucial.

To relate optical density of the image to exit dose to air or air kerma of the compressed breast or phantom, a correction has to be made for production of scattered radiation followed by absorption in the anti-scatter grid.

Although not a true validation of the method, the known thickness estimation of a 4 cm thick PMMA phantom from the optical density of the film is encouraging.

The breast model in which the skin and underlying layer of adipose tissue were simulated by 5 mm of adipose tissue appeared preferable over simulation by glandular tissue.

For the study on 478 images at a relatively modern unit it appeared that in approximately 93% of the cases the glandularity was in the range of 0 to 1.

The average compressed breast thickness is approximately 5.5 cm and 95% of the compressed breast thicknesses are in the range of 3.5 to 8 cm.

The automatic selection of the Mo or the Rh filter seems to function properly, and consequently a dose reduction can be expected, e.g., Klein *et al* (1995).

The average value of the mean glandular dose at the mammography unit as well as the standard deviation seems reasonable.

Acknowledgment

This work was supported in part by the Dutch ‘College voor Zorgverzekeringen’ (Health Care Insurance Board), previously ‘Ziekenfondsraad’ in a project entitled ‘Stralingsbelasting bij het bevolkingsonderzoek naar borstkanker in Nederland’.

References

Beckers S W, Schutten M C, Geertse T D, Bijkerk K R, van Engen R E, Oostveen L J and Swinkels M M J 2003 *Results of Technical Quality Control in the Dutch Breast Cancer Screening Programme (2001–2002)* (Nijmegen: National Expert and Training Centre for Breast Cancer Screening (LRCB))

Berger M J and Hubbell J H 1999 *XCOM Documentation* (Gaithersburg, MD: National Institute of Standards and Technology (NIST))

Briesmeister J F 2000 *MCNP—A General Monte Carlo N-Particle Transport Code* (Los Alamos, NM: Los Alamos National Laboratory) Manual LA-13709-M, version 4C

Burch A and Law J 1995 A method for estimating compressed breast thickness during mammography *Brit. J. Radiol.* **68** 394–9

Dance D R 1990 Monte Carlo calculation of conversion factors for the estimation of mean glandular breast dose *Phys. Med. Biol.* **35** 1211–9

Dance D R, Skinner C L, Young K C, Beckett J R and Kotre C J 2000 Additional factors for the estimation of mean glandular breast dose using the UK mammography dosimetry protocol *Phys. Med. Biol.* **45** 3225–40

Hammerstein G R, Miller D W, White D R, Masterson M E, Woodard H Q and Laughlin J S 1979 Absorbed radiation dose in mammography *Radiology* **130** 485–91

Highnam R and Brady M 1999 *Mammographic Image Analysis* (Dordrecht: Kluwer)

Highnam R P, Brady J M and Shepstone B J 1998 Estimation of compressed breast thickness during mammography *Brit. J. Radiol.* **71** 646–53

Hubbell J H, Veigele W m J, Briggs E A, Brown R T, Cromer D T and Howerton R J 1975 Atomic form factors, incoherent scattering functions, and photon scattering cross sections *J. Phys. Chem. Ref. Data* **4** 471–538

ICRU (International Commission on Radiation Units and Measurements) 1989 Tissue substitutes in radiation dosimetry and measurement *ICRU Report 44* (Bethesda, MD: ICRU)

ICRU (International Commission on Radiation Units and Measurements) 1992 Measurement of dose equivalents from external photon and electron radiations *ICRU Report 47* (Bethesda, MD: ICRU)

IPEM (Institute of Physics and Engineering in Medicine) 1997 Catalog of diagnostic x-ray spectra & other data *IPEM Report 78* (York: IPEM)

Jain A 1989 *Fundamentals of Digital Image Processing* (Englewood Cliffs, NJ: Prentice-Hall) chapter 9

Johns P C and Yaffe M J 1987 X-ray characterization of normal and neoplastic breast tissues *Phys. Med. Biol.* **32** 675–95

Karssemeijer N 1998 Automated classification of parenchymal patterns in mammograms *Phys. Med. Biol.* **43** 365–78

Klein R, Aichinger H, Dierker J, Jansen J T M, Joite-Barfuß S, Säbel M, Schulz-Wendtland R and Zoetelief J 1997 Determination of average glandular dose with modern mammography units for two large groups of patients *Phys. Med. Biol.* **42** 651–71

NIST (National Institute of Standards and Technology) 1995 X-ray mass attenuation coefficients *NISTIR Report 5632* (Gaithersburg, MD: NIST)

Yaffe M and Boyd N 2005 Mammographic breast density and cancer risk: The radiological view *Gynecol. Endocrinol.* (Suppl. 1) **21** 6–11